THE ASTROPHYSICAL JOURNAL, 452:680–684, 1995 October 20

HUBBLE SPACE TELESCOPE OBSERVATIONS OF THE SN 1987A TRIPLE RING NEBULA

CHRISTOPHER J. BURROWS,[1,2] JOHN KRIST,[1] J. JEFF HESTER,[3] RAGHVENDRA SAHAI,[4] JOHN T. TRAUGER,[4]
KARL R. STAPELFELDT,[4] JOHN S. GALLAGHER III,[5] GILDA E. BALLESTER,[6] STEFANO CASERTANO,[7]
JOHN T. CLARKE,[6] DAVID CRISP,[4] ROBIN W. EVANS,[4] RICHARD E. GRIFFITHS,[7]
JOHN G. HOESSEL,[5] JON A. HOLTZMAN,[8] JEREMY R. MOULD,[9]
PAUL A. SCOWEN,[3] ALAN M. WATSON,[5]
AND JAMES A. WESTPHAL[10]

Received 1994 October 11; accepted 1994 December 22

ABSTRACT

We have observed SN 1987A with the optically corrected WFPC2 on the *Hubble Space Telescope* both in emission lines and in the UV and optical continuum. The previously observed outer nebular structure is shown to be part of two closed unresolved loops. These loops were flash-ionized by the supernova itself. They are not caused by limb brightening of an hourglass shell produced by the interaction of the winds from the progenitor. The inner ring is seen to be extended and may be connected to the new outer rings by sheets of material. However, beyond the outer rings, emission is not seen, implying a very low density ($n < 10$) for the outer hourglass shell if it exists. The new outer rings are unresolved, and this together with their observed brightness implies a density $n > 1000$. This density contrast of at least 100 is difficult to reconcile with the conventional picture of the progenitor evolution. Two models for the rings are presented, but each is deficient in important respects. A proper understanding of this system will require new physical insight.

Subject headings: ISM: bubbles — ISM: jets and outflows — shock waves — stars: mass loss — supernovae: individual (SN 1987A)

1. INTRODUCTION

SN 1987A in the Large Magellanic Cloud is surrounded by a complex nebula, consisting of an elliptical-shaped central ring and an outer structure which looks from the ground like two arcs displaced north and south from the central ring. This outer nebula at $\sim 2''$ from SN 1987A was first observed in 1989 March (Crotts, Kunkel, & McCarthy 1989). It was seen both in emission and continuum light and interpreted as a light echo. Significantly, the southern arc was not completely visible then, which we interpret as due to its not yet having been illuminated by the SN flash. This contradicts the interpretation given by Wang & Wampler (1992), who considered that all of the structures that make up the two nebular loops were within the light-travel paraboloid of the SN by 1989 March. Subsequent observations (Wampler et al. 1990) on 1989 December 26 showed the complete structure to the south. The lack of any apparent motion of the arcs over this and subsequent *Hubble Space Telescope* (*HST*) (Plait et al. 1995) and ground-based images showed that they are not light echos. They must be understood to be an essentially stationary emission-line nebula which was flash-ionized by the SN explosion itself. From the delay in illuminating the southern edge of the outer nebula we deduce that it is just behind (within 9 lt-months of) the plane of the sky. We also conclude that the structure was not ionized prior to the SN explosion. None of the outer loop structure is visible in preexplosion plate material (Walborn et al. 1987), which probably lacked the sensitivity to see it, or in coronagraphic observations in 1988 (Paresce & Burrows 1989).

The standard interpretation (Kahn & West 1985; Wampler et al. 1990; Luo & McCray 1991; Wang & Mazzali 1992; Blondin & Lundqvist 1993) of the outer and inner nebulae involves an interaction between the stellar winds from two phases of the progenitor. In this model, a fast tenuous blue supergiant (BSG) wind runs into a slow dense red supergiant (RSG) wind which has a higher density in the equatorial plane than along the polar direction. The BSG wind sweeps up the RSG wind into a hourglass-shaped shell. This shell is then ionized by the UV flash from the SN to produce the structures that we see. High-density gas in the shell at the "waist" of the hourglass produces the inner ring, whereas limb brightening of the two lobes of the hourglass is supposed to create the outer rings. The inner nebulosity discussed here is to be distinguished from the outer (Crotts 1988) and inner (Bond et al. 1989; Chevalier & Emmering 1988; Sparks, Paresce, & Macchetto 1989) echoes which are caused by scattering on the interstellar medium (ISM) and RSG wind, respectively.

We present WFPC2 images of the nebula around SN 1987A, which show that the outer nebula cannot be explained by this standard interacting-winds model. It is seen to consist of two complete thin loops of material. The loops are too bright and thin for limb brightening to explain their appearance. Furthermore, whatever the source of the loops, the expected shell itself is not seen.

[1] Space Telescope Science Institute, 3700 San Martin Drive, Baltimore, MD 21218.
[2] Also Astrophysics Division, Space Science Department, European Space Agency.
[3] Department of Physics and Astronomy, Arizona State University, Tyler Mall, Tempe, AZ 85287.
[4] Jet Propulsion Laboratory, 4800 Oak Grove Drive, Pasadena, CA 91109.
[5] Department of Astronomy, University of Wisconsin—Madison, 475 North Charter Street, Madison, WI 53706.
[6] Department of Atmospheric and Oceanic Sciences, University of Michigan, 2455 Hayward, Ann Arbor, MI 48109.
[7] Department of Astronomy, Johns Hopkins University, 3400 North Charles Street, Baltimore, MD 21218.
[8] Lowell Observatory, Mars Hill Road, Flagstaff, AZ 86001.
[9] Mount Stromlo and Siding Springs Observatories, Australian National University, Weston Creek Post Office, ACT 2611, Australia.
[10] Division of Geological and Planetary Sciences, California Institute of Technology, Pasadena, CA 91125.

2. OBSERVATIONS

The refurbished *HST* was used to take images with the WFPC2 planetary camera, both in emission lines Hα(λ6563) + [N II](λ6548) and [O III](λ5007) and in the optical and UV continuum (5470 and 2550 Å). The images taken are summarized in Table 1 and, after standard reduction to remove cosmic rays, hot pixels, and bias level are shown in Figure 1 (Plate 21).

The imaging of the "outer arcs" as parts of two transversely unresolved complete ring structures is clearly inconsistent with the conventional model. Although we have successfully reproduced the observed morphology of three intersecting rings by limb-brightening a model hourglass-shaped shell with an equatorial density enhancement, the rings observed by *HST* are much too thin, and quantitative comparisons fail. One way to see this is to compare the azimuthal average profile of a portion of one ring with what one would expect from limb brightening. The sharpest profile one can obtain would be from a shell that is much thinner than the instrumental resolution. At a distance d from the limb of such a shell, one gets an intensity that falls off as $1/d^{1/2}$ (convolved with the instrumental response), provided d is much less than the local curvature. In the case of interacting wind-blown bubbles, the curvature, density, and thickness of the shell will be locally constant near the limb (at least over most of the length of the arcs) for any reasonable geometry. By locally constant, we mean constant over a distance that is large compared to the resolution element but small compared to the overall nebula. In Figure 2 a comparison is made between the measured profile of one of the arcs, the predicted profile for a limb-brightened thin spherical shell, and the instrumental response. It can be seen that the data do not fit the limb-brightening prediction at all. The above general argument shows that close to the limb, the brightness distribution is independent of the geometry, so no limb-brightened model can fit the data. On the other hand, the data do appear to be almost exactly what one would expect from an unresolved line source. We conclude that the outer nebula is a pair of real ring structures in which the density is significantly enhanced relative to the surroundings and is not caused by line-of-sight projection through a more tenuous nebula.

A natural interpretation of the image is that the three rings lie in three planes roughly perpendicular to the same axis through the SN and are all therefore inclined to our line of sight by roughly the same angle. The inner loop is known to be inclined to the line of sight by ~43°. Observations of the inner loop have shown that it has a radial velocity of ~7 km s^{-1} (Wampler & Richichi 1988; Crotts & Heathcote 1991), corresponding to radial expansion or contraction at 10.3 km s^{-1}. If we assume that the inner ring is in fact expanding, then the northern edge of the inner loop is tilted toward us. In that case, the southern arc that was lit up last by the explosion represents the back of the loop nearest us. It has already been shown to be

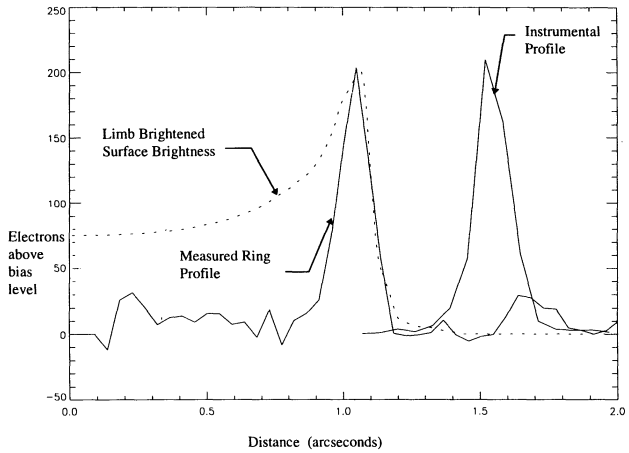

FIG. 2.—Azimuthal average of the intensity of the southern edge of the nebula relative to its local center of curvature, compared to the expected form for limb brightening, normalized to the same peak position and count rate, and to the instrumental profile expected for a transversely unresolved source.

just behind but within 9 lt-months of the plane of the sky through the SN. The more perfectly elliptical northern loop is then generally behind the other two loops, with its closest northern edge in the plane of the sky or closer. The SN remnant itself is projected onto the back of the northern loop. These geometric constraints imply that the rings subtend at least 90° at the SN. Maximum radial velocity measurements of 22.5 km s^{-1} on the outer nebula are somewhat smaller than one would expect from Blondin & Lundqvist (1993; Cumming 1994). The possible geometry for the object that we infer from the WFPC2 images, radial velocity measurements, and timing considerations is shown in Figure 3.

The inner and outer rings may be connected by a low surface brightness wall that fades rapidly away from the inner ring. This wall would account for the detected diffuse emission which lies between the rings and is particularly bright where the line of sight is close to tangential to conical surfaces connecting the inner and outer rings. This material is most visible along and near the minor axis of the inner rings, which means that it is probably not coplanar with it. If it were, it would have to be distributed in a nonaxisymmetric manner. There is no evidence for any extended emission (apart from the SN remnant and the back of the north loop) inside the inner ring. All of the emission that is visible in Figure 1 in that region can be explained by the instrumental point-spread function (PSF). The data do not show a closed bubble structure further out from the SN than the location of the rings. Bounds on the density of such a surface are discussed below.

Many of these observations are most obvious in a maximum entropy deconvolved F656N image as shown in Figure 4 (Plate 22), which clearly shows the extended emission attached to the

TABLE 1

SUMMARY OF OBSERVATIONS

Filter	Wavelength (Å)	Width (Å)	Efficiency	Peak Transmission	Number of Exposures	Total Exposure (s)
F255W.....	2609	422	0.00085	0.00461	2	2400
F502N	5013	27	0.00036	0.0504	2	2400
F547M.....	5478	486	0.01223	0.103	2	2400
F656N	6564	21	0.00053	0.124	2	2400

PLATE 21

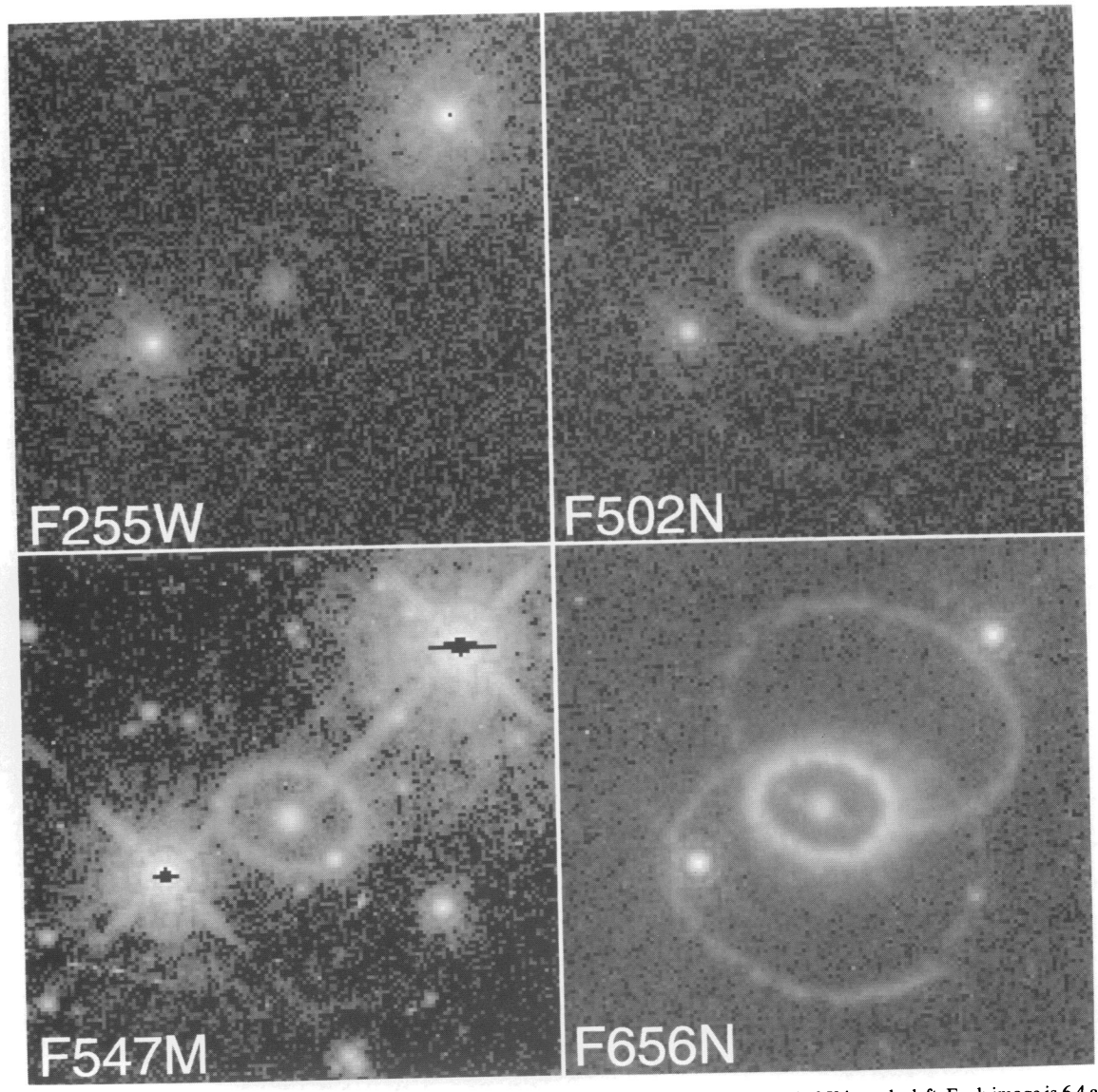

FIG. 1.—*HST* planetary camera images of SN 1987A taken in 1994 February. Up is at P.A. 5°, and P.A. 95° is to the left. Each image is 6.4 arcsec^2.

BURROWS et al. (see 452, 681)

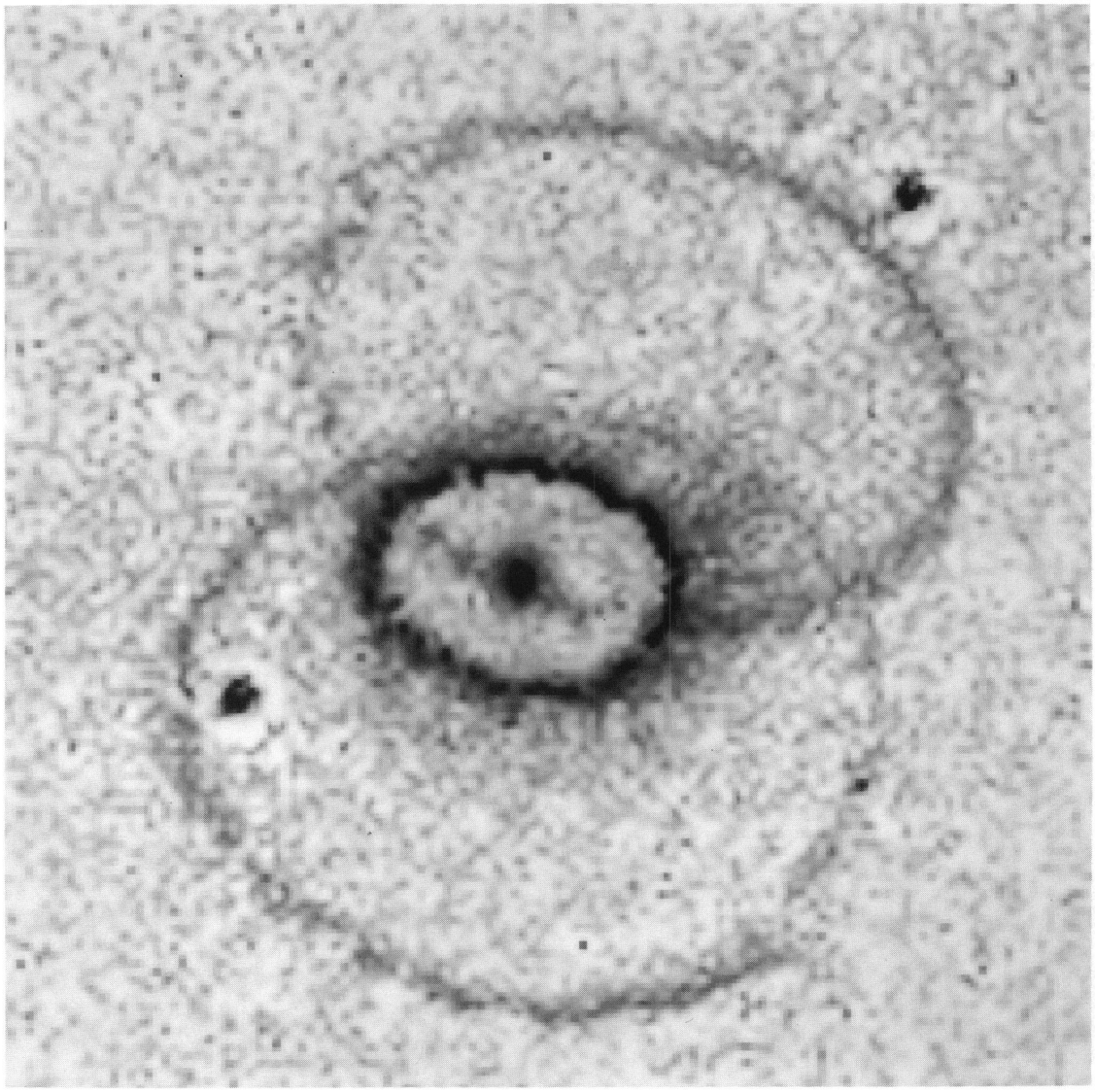

FIG. 4.—Deconvolved F656N image, at the same orientation as Fig. 1. The image is 5.8 arcsec^2.

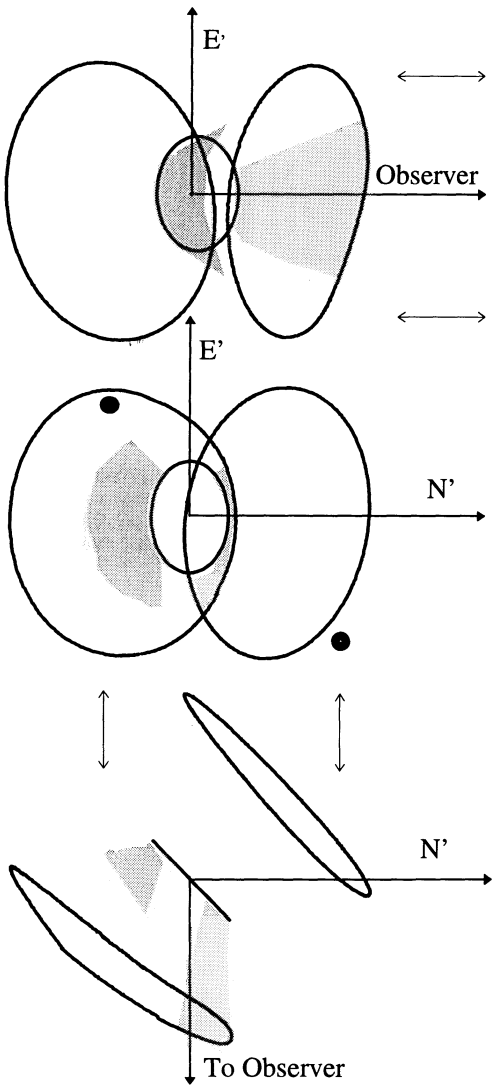

FIG. 3.—Geometry for the three rings that is consistent with the new images, and light-travel time constraints. Hypothetical sources for the extended emission seen in the images are also marked.

outside of the inner ring and the thinness of the outer rings. The outer rings are resolved only at one short section on each, where they may not quite close on themselves. The resolved sections are almost diametrically opposite each other at position angles from the supernova of about 30° on the northern ring and 210° on the southern ring, and are ~0.″5 long.

We have measured the eccentricities, position angles, and count rates of the rings, and these data are summarized in Table 2. The south ring is not an ellipse, because the radii of curvature at either end of its long axis are markedly different. In Table 2, the width given is the width of a mask used, centered on a geometric ellipse as specified, to include most of the light from each ring. It therefore allows for instrumental broadening, as well as the fact that the rings are not perfect ellipses. As observed above, the rings themselves are unresolved. The center of the inner ring is at the SN. However, the line joining the centers of the outer rings misses the SN by ~0.″4.

TABLE 2

GEOMETRIC AND PHOTOMETRIC PARAMETERS OF THE THREE RINGS

	Northern Outer Ring	Southern Outer Ring	Inner Ring
Eccentricity	0.678	0.513	0.711
Semimajor axis (arcsec)	1.77	1.84	0.81
Semiminor axis (arcsec)	1.30	1.58	0.57
P.A. of major axis	70.7	90.0	81.2
Width (arcsec)	0.37	0.36	0.37
Area included (arcsec^2)	2.97	3.57	1.31
Area excluded (arcsec^2)	0.52	0.69	0.15
F255W magnitude	18.91	19.65	20.08
F502N magnitude	17.51	17.79	16.56
F547M magnitude	19.55	19.89	19.73
F656N magnitude	16.10	16.14	14.31

A star appears in projection on each ring. We believe this to be a coincidence, but they may be helpful in modeling, interpreting, or diagnosing the rings. We therefore give in Table 3 flux measurements for each of these stars, as well as for stars 2 and 3 which were seen in preexplosion plates (Walborn et al. 1987). The flux quoted was measured with a 5 pixel aperture with an assumed constant background and will therefore include some light from the neighboring ring. The efficiencies from Table 1 have been used in accordance with equation (6.1) in Burrows (1994) to give Oke magnitudes which are directly related to flux density. The F255W observation of star 2 had one saturated pixel, and the F547M observations of stars 3 and 2 had 14 and 36 saturated pixels, respectively. For the purposes of computing a flux, each saturated pixel was assumed to contribute 100,000 electrons. This method of dealing with saturated pixels has been shown in Gilliland (1994) to give reasonable results (there is also a discussion of the errors implied by it).

3. INTERPRETATION

Many qualitative and quantitative features of the *HST* data cannot be explained in the context of the best preexisting models. The aim of this section is to bring out the new discrepancies between the models and the data. We have already discussed the fact that the rings are unresolved, and the problems that this implies for the limb-brightening model. Now we assume that the rings are instabilities or density enhancements in an interacting-winds shell. We emphasize the very high contrast between the rings and the surrounding shell that this implies. This contrast places severe constraints on any attempt to model the rings by hydrodynamic interactions of precursor winds.

For purposes of illustration, we take the wind model parameters from Table 1 of Blondin & Lundqvist (1993), which represents the most sophisticated quantitative representation of the interacting-winds hypothesis. Most other authors have also

TABLE 3

OBSERVED OKE MAGNITUDES (= $-2.5 \log (fv) - 48.6$) OF THE STARS ASSOCIATED WITH SN 1987A AND OF FIELD STARS THAT APPEAR ON THE RINGS

	SN 1987A	Star A	Star B	Star 3	Star 2
F255W	19.97	22.41	24.14	16.35	15.30
F502N	19.01	18.81	19.86	16.20	15.09
F547M	19.59	20.26	19.75	16.49	15.61
F656N	16.44	16.62	19.25	15.40	15.38

used similar wind parameters. We therefore assume a RSG mass-loss rate $\dot{M}_R = 1 \times 10^{-5}\ M_\odot\ \mathrm{yr}^{-1}$ at velocity $v_R = 10$ km s^{-1} and a BSG mass-loss rate $\dot{M}_B = 2 \times 10^{-6}\ M_\odot\ \mathrm{yr}^{-1}$ at velocity $v_B = 550$ km s^{-1}. These parameters imply an expansion rate of the outer shell of order 85 km s^{-1}, which is perhaps consistent with the measured much smaller radial velocity of the outer rings, when the positions at which they were measured best is noted to be close to the plane of the SN in the sky. The inner ring, corresponding to the waist of the hourglass, is observed to be expanding at a deprojected rate of 10.3 km s^{-1}, which gives a dynamical bound on the lifetime of the BSG phase of 20,000 yr.

Using these parameters, we can show that the shell would be substantially ionized by the initial 10^{57} ionizing photon UV flash from the SN. The radius of the outer shell should be of order 5×10^{18} cm, which is still well within the RSG wind envelope of order 3×10^{19} cm (and within the unshocked region if the Napoleon's Hat Nebula to the north of the SN is interpreted as the RSG wind–ISM bow shock.). This would imply a total swept-up mass in the shell of $\sim 1.7\ M_\odot$ with a column density of 5.6×10^{18} cm^{-2}. Twice the observed ionizing photon flux from the SN would completely ionize the shell. As a rough check, these RSG wind parameters imply 1.5 $M_\odot$ in the unperturbed wind between 3 and 8 lt-yr from the SN. Crotts & Kunkel (1991) derived a somewhat lower 0.34 $M_\odot$ from the observed grain scattering with an assumed dust-to-gas ratio of 1000.

We do not observe the limb-brightened shell, except close to the inner ring, and this enables us to derive a bound on the density in the outer lobes. We have added simulated projected hourglass-shaped shells convolved with the instrumental response to the data. We find that a total signal of 10^5 photoelectrons in shells ranging in length from the size of the outer rings to twice their size can be clearly seen in the data. This signal level corresponds to a flux from the shell of 2.4×10^{45} Hα photons s^{-1}—15% less than the outer rings. A signal of half this size would probably not be seen, and therefore we regard this signal level as a bound on the brightness of the shell. The projected 1.7 $M_\odot$, if fully ionized, would need to be distributed at a density of 5 cm^{-3} (with a resulting recombination time of 2.3×10^4 yr) to give this signal level. Even if the shell is partially neutral, nebular emission will resonantly scatter out of the nebula immediately. We conclude that for the standard interacting wind parameters, the density in the shell is less than 5 and the compression of the RSG wind implied is a factor of less than 5, or most of the nebula was not ionized. A strong shock compresses an adiabatic gas by a factor of 4 without radiative cooling, and hydrodynamic models have much higher compression ratios if there is time for significant cooling.

We can derive another density bound for the shell without assuming a total mass if, instead, we assume that the shell thickness is 3×10^{16} cm, which is a typical nebular cooling scale (and also corresponds to our pixel size). In this case, the density is given as $n_e = (F/\alpha V_{\mathrm{shell}})^{0.5} \leq 28$ cm^{-3}, where F is the bound on total Hα flux from the shell. This implies a total mass in the shell of only 0.3 $M_\odot$. Thus the fact that the outer lobes are not seen represents a significant problem for the interacting-winds models.

On the other hand, we can compute a similar lower bound on the density in the rings from the fact that they are unresolved. If the emitting region is less than 1 pixel in width and depth (the structures are presumably inclined at $\sim 45°$ to the line of sight), we derive an emitting volume $V_{\mathrm{ring}} < 1.1 \times 10^{52}$ cm^3. The density is given as $n_e = (F/\alpha V)^{0.5} \geq 1000$ cm^{-3}, where in this case F is the measured total Hα flux from the region. The mass in each ring is less than 0.008 $M_\odot$ (0.005 of the total expected in the shell), but this material has been compressed by more than a factor of 100 compared to the rest of the material that was presumed to be in the shell.

It is possible to very roughly estimate the average density ratio between the possible connecting wall and the rings. We begin by comparing the brightness of the rings with the brightness of the diffuse emission. The rings have an average brightness per unit length of 2.3×10^{-15} ergs cm^{-2} s^{-1} arcsec^{-1}. The diffuse emission between the inner and outer ring has a rough average surface brightness of $\sigma = 3 \times 10^{-14}$ ergs cm^{-2} s^{-1} arcsec^{-2}. If the wall is being viewed at an angle θ from its tangent, then the average face-on surface brightness of the cavity wall is $\sigma \sin\theta$. Estimating $\theta = 14°$ from Figure 3 gives a value for the average face-on surface brightness of the wall of 3×10^{-15} ergs cm^{-2} s^{-1} arcsec^{-2}. As is apparent from the image, the diffuse emission is significantly brighter near the inner ring than near the outer ring. If the wall thickness is equal to the ring thickness (0.″05 = 3.8×10^{16} cm is roughly the cooling length behind a radiative shock in gas with a density of a few particles per cm^3) and both phases are still mostly ionized (i.e., the recombination time is $\gg 7$ yr), the density ratio between the ring and the emission-weighted average of the wall comes out ~ 4. The density of the wall where it joins the outer ring is certainly much less.

4. POSSIBLE MODELS

The most conventional models produce the observed structures by progenitor wind interactions. One possibility is that the mass loss was greater near the end of the RSG phase when the structure of the star was undergoing rapid changes. This might lead to an equatorially concentrated RSG wind in two distinct radial regions: an inner, higher density region and an outer, lower density region, separated by a thin, dense shell. When the BSG wind is turned on at the center of such a structure, it should expand into the inner dense region of the wind in two bubbles until it breaks through the dense shell. At this point, the high pressure in the bubble interior will be largely released by driving an expanding shock wave into the outer lower density wind zone. The rings would then form as density enhancements in the shell around the region of breakout. The dense shell itself may have been a discrete shell ejection event at the onset of the heavier wind phase, as in Wang & Mazzali (1991), or if the velocity of the RSG wind increases rapidly enough near the end of the RSG phase and the flow is supersonic, a Rayleigh-Taylor stable shock. With the addition of postshock cooling, this mechanism should be able to generate a factor of 10 or so density ratio between the shell and the inner wind zone.

There are three problems with this type of model: First, the interface between the two RSG wind phases is only observed in the vicinity of the BSG wind breakout and is not seen limb-brightened elsewhere. Second, the interaction between the BSG wind and the outer RSG wind is not observed. Third, there is observational (e.g., Icke, Preston, & Balick 1989) and numerical hydrodynamic (e.g., Garcia-Segura & Mac Low 1994) evidence from studies of other objects that would lead one to expect filamentary instabilities associated with the breakout. One possible way out of some of these objections is by shadowing of the ionizing flux by inner regions of the nebula, but this

seems rather artificial. Without detailed hydrodynamic simulations, it is unclear whether any interacting wind model can fit the observations, because of the extreme density variations that must be generated and sustained in the flow and the lack of other structures that one might expect to observe.

A more radical wind-based model for the outer loops has been proposed by Podsiadlowski, Fabian, & Stevens (1991). In this interpretation, interacting winds from a binary companion and the progenitor are swept up to form a truncated double cone. We find that this model has difficulty explaining the emission seen between the rings.

Another radical idea is that the two outer rings are produced by the action of a bipolar, highly collimated, precessing jet. The gross symmetry of the nebula about a point close to the progenitor, and the way in which the two loops do not seem to exactly close on each other at diametrically opposite points, provide support for this idea. The jet is supposed to strike the hourglass walls and compress the material there. The accretion disk driving the jet might have been produced by gravitational capture of some of the progenitor's RSG wind by a compact secondary companion. The disk augments the accretion by acting as a barrier to outflowing matter which would otherwise be lost from the system, accelerating its growth until its radius approaches that of the Roche lobe of the secondary. Such a model has been proposed by Morris (1987) to explain the distinctive morphological features of bipolar pre–planetary nebulae (PPNs). The production of the bipolar jet in Morris's model is assumed to be analogous to that occurring in protostellar environments (e.g., Pudritz & Norman 1983) and is driven by the rotational energy of the disk around the companion star, in the presence of a magnetic field. The analogy with the protostellar environment is particularly apt, since the "ansae" seen in Planetary nebulae (PNs) are very similar to the Herbig-Haro objects seen in protostellar environments and thought to be produced by jets interacting with ambient material. The point symmetric nature of the circumstellar structure in PPNs and PNs is explained by wobbling of the disk/jet axis. However, the operation of the jetlike outflow in PNs and SN 1987A cannot be entirely similar, since with one exception (MyCn 18), PNs do not show the outer ring structures seen in the latter. Thus, whereas in PNs, the jet axis is not required to make a complete precessional orbit, it must do so in SN 1987A in order to create the outer rings. A major difficulty with this model is the small radial expansion velocity of the outer rings. It is hard to see how the gas in the outer walls can be compressed enough without significant momentum transfer taking place.

Binarity for the progenitor is a natural method of producing the equatorially concentrated RSG wind which is required to explain the inner ring in all models. It has also been suggested from other considerations, including the large overabundance of N (Fransson et al. 1989) in SN 1987A's circumstellar gas and possibly He in circumstellar (Allen, Meikle, & Spyromilio 1989) and SN gas (Eastman & Kirshner 1989). The transfer of angular momentum to Sk -69° 202 during close binary evolution may provide the mixing required to bring He and N from the core to the outer envelope (Chevalier 1992).

In conclusion, we have shown the outer nebula surrounding SN 1987A is a pair of thin rings, but it is going to be very difficult to explain them without some new physical ideas.

This study was partially funded by the WFPC2 Investigation Definition Team (NASA contract NAS7-1260). The study was based on observations with the NASA/ESA *Hubble Space Telescope*, obtained at the Space Telescope Science Institute, which is operated by the Association of Universities for Research in Astronomy, Inc., under NASA contract NAS5-26555.

REFERENCES

Allen, D. A., Meikle, W. P. S., & Spyromilio, J. 1989, Nature, 342, 403
Blondin, J. M., & Lundqvist, P. 1993, ApJ, 405, 337
Bond, H. E., Gilmozzi, R., Meakes, M., & Panagia, N. 1990, ApJ, 354, L49
Burrows, C. J. 1994, WFPC2 Instrument Handbook, Version 2.0 (Baltimore: STScI)
Chevalier, R. A. 1992, Nature, 355, 691
Chevalier, R. A., & Emmering, R. T. 1988, ApJ, 331, L105
Crotts, A. P. S. 1988, ApJ, 333, L51
Crotts, A. P. S., & Heathcote, S. R. 1991, Nature, 350, 683
Crotts, A. P. S., & Kunkel, W. E. 1991, ApJ, 366, 73
Crotts, A. P. S., Kunkel, W. E., & McCarthy, P. J. 1989, ApJ, 347, L61
Cumming, R. J. 1994, Ph.D. thesis, Univ. London
Eastman, R. G., & Kirshner, R. P. 1989, ApJ, 347, 771
Fransson, C., et al. 1989, ApJ, 336, 429
Garcia-Segura, G., & Mac Low, M. 1994, in Proc. 34th Herstmonceux Conf., ed. R. E. S. Clegg & I. R. Stevens (Cambridge: Cambridge UniversityPress), 85
Gilliland, R. 1994, ApJ, 435, L63
Icke, V., Preston, H. L., & Balick, B. 1989, AJ, 97, 462
Kahn, F. D., & West, K. A., 1985, MNRAS, 212, 837
Luo, D., & McCray, R. 1991, ApJ, 379, 659
Morris, M. 1987, PASP, 99, 1115
Paresce, F., & Burrows, C. 1989, ApJ, 337, 13
Plait, P. C., Lundqvist, P., Chevalier, R. A., & Kirshner, R. P. 1995, ApJ, 439, 730
Podsiadlowski, P., Fabian, A. C., & Stevens, I. R. 1991, Nature, 354, 43
Pudritz, R. E., & Norman, C. A. 1983, ApJ, 274, 677
Sparks, W. B., Paresce, F., & Macchetto, D. 1989, ApJ, 347, 65
Walborn, N. R., Lasker, B. M., Laidler, V. G., & Chu, Y. H. 1987, ApJ, 321, 41
Wampler, E. J., & Richichi, A. 1989, A&A, 217, 31
Wampler, E. J., Wang, L., Baade, D., Banse, K., D'Odorico, S., Gouiffes, C., & Tarenghi, M. 1990, ApJ, 362, 13
Wang, L., & Mazzali, P. A. 1991, A&A, 241, 17
———. 1992, Nature, 355, 58
Wang, L., & Wampler, E. J. 1992, A&A, 262, L9